J. Indones. Math. Soc.
Vol. 31, No. 02 (20x25), pp. 1–10.

Fourth Order PDE: Model of Thin Film Flow Involving Surface Tension

Leo Hari Wiryanto[1*], Warsoma Djohan[1]

[1] **Faculty of Mathematics and Natural Sciences, Institut Teknologi Bandung, Indonesia,**

wwwiryanto@yahoo.co.id, warsoma.djohan@gmail.com

Abstract. Surface wave on thin film is considered by involving surface tension. The fluid flows on an inclined channel. The model is based on lubrication theory, and presented in a single equation of the thickness of the fluid as wave movement, and the equation is strongly nonlinear. In solving the model, scaling and linearized processes are applied. So that three physical parameters play an important role in the wave propagation: bottom inclination, length of the scaling and the surface tension. Each of those parameters is represented as a term in the equation. Then, the equation is solved numerically by an implicit finite difference method for the linearized equation, so that the solution can be used to observe the effect of those physical quantities. We found that the surface wave propagates with different speed and reducing the amplitude. When the surface tension is involved, the profile of the wave slightly changes, beside it also effect to the movement of the wave. This is simulated in this paper.

Key words and Phrases: thin film flow, surface tension, implicit finite difference method, Gauss-Seidel iteration

1. INTRODUCTION

A 2-D thin film flow is modeled from lubrication theory subject to the boundary conditions. The fluid is on an inclined channel, so that the gravitational and pressure forces play an important role in the formulation of the fluid flow, presented in term of the fluid thickness h, depending on the position x and time t. Physically, this thickness variable represents surface wave propagating satisfying the equation deriving from the governing equation.

*Corresponding author

2020 Mathematics Subject Classification: 76A20, 76D08, 76M20
Received: 04-07-2023, accepted: 20-10-2024.

As the reference of the lubrication theory, we can see such as in Pozrikidis [1] and Bachelor [2]. Wiryanto and Febrianti [3] used that theory as the governing equation of the thin film flow. Together with the boundary conditions, they formulated the problem into an unsteady single equation of the fluid depth h. Similarly, King, et. al. [4] formulated a steady thin viscous flow with air-blown above the fluid. When the surface tension is considered, it can be expressed to the pressure at the surface. The normal stress can be approximated with the negative of the pressure, yielding the pressure jump condition. Therefore, the pressure at the surface is the atmospheric, chosen as the reference, and the multiplication between the surface tension and the curvature of the sloped free surface. The model in [3] must be added a term containing a third derivative of fluid depth. This model is our concern to study. The derivation of this equation can be seen in Wiryanto, et. al. [5].

Since the model is strongly nonlinear. In this paper we propose to solve the problem for linearized one, and solved numerically by an implicit finite difference. This is developed from Putra, et. al. [6], who worked the similar problem without involving surface tension. Putra, et. al. [6] analyzed the numerical method, and found that the method is unconditional stable. An explicit method was applied for the problem in Wiryanto, et. al. [5], and they found the method was conditional stable. Similar explicit method and its stability had been studied by Wiryanto in [7] and [8]. Moreover, the explicit method was unable to show the effect of the surface tension, because of the numerical stability reason. To solve that problem, here we introduce scaling to the variables before we solve the equation.

2. PROBLEM FORMULATION

A thin film flow is our concern. The sketch of the flow is shown in Figure 1. The fluid depth is h, measured from the bottom of the channel, inclined with small angle θ. So that we can see the effect of gravity to the pressure in both directions of the coordinates. We choose the horizontal coordinate x along the channel and the vertical one y is perpendicular to the other. So that, the gravitational force is projected to each coordinate and related to the pressure satisfying momentum conservation. Following Wiryanto, et. al. [5], the lubrication theory is mass conservation, presented as equation of the vertical and horizontal velocities, and its momentum one.

Those governing equations subject to the bottom and surface boundaries are then solved to get a single equation of h. At the surface, the pressure is

$$P_{fs} = P_{atm} + \gamma\kappa$$

where P_{atm} is the atmospheric pressure, we choose as the reference; γ is the surface tension and $\kappa \approx -\frac{\partial^2 h}{\partial x^2}$ is the curvature of sloped free surface. By this pressure, model in [3] becomes

$$h_t + \frac{\rho g}{3\mu}\left[h^3\left(\sin\theta - h_x\cos\theta + \frac{\gamma}{\rho g}h_{xxx}\right)\right]_x = 0 \qquad (1)$$

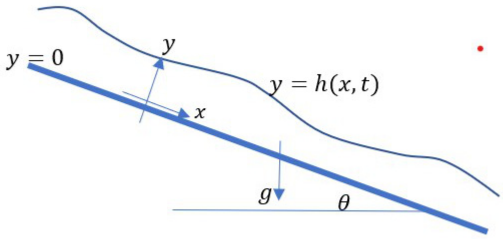

FIGURE 1. Sketch of the flow and the coordinates.

The last term in (1) is added as the effect of the surface tension. Here we use conventional physical notations. The derivation of (1) can be seen in [5], and it was solved numerically by explicit finite difference method forward time cental space. The method was unable to calculate the problem for relatively large of the surface tension γ, because of the stability reason. Meanwhile, in case of surface tension neglected, the numerical scheme should be run with small time step, and the wave movement was very slow. These difficulties bring us to work in this paper by scaling the variables and to choose an implicit method but for linearized model.

In obtaining the linearized equation, suppose h_0 is constant solution, i.e. fluid depth without any disturbance. When we write

$$h = h_0 + \epsilon\eta$$

for small parameter ϵ, the first order of (1) is linear equation

$$\eta_t + \frac{\rho g}{\mu} h_0^2 \sin\theta \eta_x - \frac{\rho g}{3\mu} h_0^3 \cos\theta \eta_{xx} + \frac{\gamma h_0^3}{3\mu} \eta_{xxxx} = 0.$$

Now, we scale the variables by

$$\bar{x} = \frac{x}{L}, \bar{\eta} = \frac{\eta}{h_0}, \bar{t} = \frac{t}{\tau} \tag{2}$$

where L is wavelength, and $\tau = \frac{\mu L}{\rho g h_0^2}$. By this scaling, the simulation of $\bar{\eta}(\bar{x}, \bar{t})$ is fast motion of $\eta(x,t)$, since τ is proportional to $L >> 1$, and the linear equation above becomes, written without bar $(\bar{.})$,

$$\eta_t + a\eta_x + b\eta_{xx} + c\eta_{xxxx} = 0. \tag{3}$$

The coefficient of each term is

$$a = \sin\theta, b = -\frac{1}{3} r \cos\theta, c = \delta r.$$

We use $r = h_0/L$ and $\delta = \gamma/(3\rho g L^2)$. Physically, this process gives a model that can handle the difficulties in movement and observing the surface tension expressing in parameter δ.

Now, we consider a monochromatic solution of (3). Suppose it is a wave having wave-number k and frequency in complex form $\omega = \omega_r + i\omega_i$, so that the solution is

$$\eta(x,t) = Ae^{\omega_i t}e^{i(kx-\omega_r t)}$$

with amplitude depending on time $Ae^{\omega_i t}$ for constant A. Here, we use notation $i = \sqrt{-1}$. Those parameters of the wave are our concern relating to (3). We substitute that type of solution into (3). The real and imaginer parts are

$$\omega_i + ck^4 - bk^2 = 0$$
$$\omega_r - ak = 0.$$

Since $b < 0$ the real part gives $\omega_i < 0$ which means the wave travels to the right by decreasing the amplitude. The second and fourth derivatives of η are influential to the amplitude. For monochromatic wave, it travels with wave speed a, and the decreasing of the amplitude is dominated by b of order k^2 followed by c of order k^4. So, surface tension is less influential then gravitational.

3. NUMERICAL PROCEDURE

Numerical method for (3) is explained in this section. A finite difference method is chosen based on forward time, average central space. We discritize time and space by $t_n = ndt$ for $n = 0, 1, 2, \cdots$ and $x_j = jdx$ for $j = 0, 1, 2, \cdots, J$, so that we can use notation $\eta_j^n \sim \eta(x_j, t_n)$. From this discitization, each derivative of η is approximated by

$$\eta_t \sim \frac{\eta_j^{n+1} - \eta_j^n}{dt}$$
$$\eta_x \sim \frac{1}{2}\left[\frac{\eta_{j+1}^{n+1} - \eta_{j-1}^{n+1}}{2dx} + \frac{\eta_{j+1}^{n} - \eta_{j-1}^{n}}{2dx}\right]$$
$$\eta_{xx} \sim \frac{1}{2}\left[\frac{\eta_{j+1}^{n+1} - 2\eta_j^{n+1} + \eta_{j-1}^{n+1}}{dx^2} + \frac{\eta_{j+1}^{n} - 2\eta_j^{n} + \eta_{j-1}^{n}}{dx^2}\right]$$
$$\eta_{xxxx} \sim \frac{1}{2}\left[\frac{\eta_{j+2}^{n+1} - 4\eta_{j+1}^{n+1} + 6\eta_j^{n+1} - 4\eta_{j-1}^{n+1} + \eta_{j-2}^{n+1}}{dx^4} + \frac{\eta_{j+2}^{n} - 4\eta_{j+1}^{n} + 6\eta_j^{n} - 4\eta_{j-1}^{n} + \eta_{j-2}^{n}}{dx^4}\right],$$

and then applied to (3), giving a system of linear equations

$$A_2\eta_{j+2}^{n+1} + A_1\eta_{j+1}^{n+1} + A_0\eta_j^{n+1} + A_{-1}\eta_{j-1}^{n+1} + A_{-2}\eta_{j-2}^{n+1} = R \tag{4}$$

where

$$R = -\left(B_2\eta_{j+2}^{n} + B_1\eta_{j+1}^{n} + B_0\eta_j^{n} + B_{-1}\eta_{j-1}^{n} + B_{-2}\eta_{j-2}^{n}\right)$$

and the coefficients

$$A_2 = \frac{c}{2dx^4}, A_1 = \frac{a}{4dx} + \frac{b}{2dx^2} - \frac{2c}{dx^4},$$
$$A_0 = \frac{1}{dt} - \frac{b}{dx^2} + \frac{3c}{dx^4}, A_{-1} = -\frac{a}{4dx} + \frac{b}{dx^2} + \frac{3c}{dx^4}, A_{-2} = \frac{c}{2dx^4},$$
$$B_2 = A_2, B_1 = A_1, B_0 = -\frac{1}{dt} - \frac{b}{dx^2} + \frac{3c}{dx^4},$$
$$B_{-1} = A_{-1}, B_{-2} = A_{-2}.$$

The equations can be solved by Gauss-Seidel iteration after giving the initial condition η_j^0 for $j = 1, 2, \cdots, J-1$, the left boundary condition at $j = -1, 0$ and the right boundary condition at $j = J, J+1$.

Before running the numerical procedure, we analyze the stability of the numerical method. To do so, we use von Neumann stability by writing

$$\eta_j^n = \xi^n e^{i\beta j}.$$

This expression is then submitted into (4), and gives

$$\xi^{n+1} = G\xi^n$$

where

$$G = \frac{-\left(B_2 e^{2i\beta} + B_1 e^{i\beta} + B_0 + B_{-1}e^{-i\beta} + B_{-2}e^{-2i\beta}\right)}{A_2 e^{2i\beta} + A_1 e^{i\beta} + A_0 + A_{-1}e^{-i\beta} + A_{-2}e^{-2i\beta}}.$$

According to the coefficients of (4) we can express the numerator as

$$\begin{aligned} &B_2 e^{2i\beta} + B_1 e^{i\beta} + B_0 + B_{-1}e^{-i\beta} + B_{-2}e^{-2i\beta} \\ &\quad = A_2 e^{2i\beta} + A_1 e^{i\beta} + B_0 + A_{-1}e^{-i\beta} + A_{-2}e^{-2i\beta}, \end{aligned}$$

and since $B_0 < A_0$ we obtain

$$\begin{aligned} &B_2 e^{2i\beta} + B_1 e^{i\beta} + B_0 + B_{-1}e^{-i\beta} + B_{-2}e^{-2i\beta} \\ &\quad < A_2 e^{2i\beta} + A_1 e^{i\beta} + A_0 + A_{-1}e^{-i\beta} + A_{-2}e^{-2i\beta}. \end{aligned}$$

The right side is the denominator of G.Therefore, the absolute value of G is less than one for any β. As the conclusion, the numerical method is stable unconditional.

4. NUMERICAL SOLUTION

Now, we solve (3) numerically by the numerical procedure described above. Most of our calculation uses homogeneous discretization space $dx = 0.1$, the same value for step time $dt = 0.1$, and the error tolerance of Gauss-Seidel iteration is upto 10^{-6}. The observation domain is $x \in (0, 100)$ divided into 1000 subintervals, for $j = 0, 1, \cdots, JJ = 1000$. Since this work mainly concerns with the surface tension, expressed in δ, so most of our simulation presents how much the effect of δ in reducing the amplitude and traveling the wave. In case $\delta = 0$ the simulation has been presented in [6]. However, the numerical method is also valid for the previous problem. Here, the system of linear equations is pentadiagonal, rather than tridiagonal in [6].

We start by solving (3) for $\theta = 5^0$, $r = 0.1$ and $\delta = 0.1$. In the observation domain $x \in (0, 100)$ the fluid surface is flat $\eta(x, 0) = 0$, and at the left side sinusoidal waves enter the domain as the left boundary

$$\eta(x,t) = 0.1 \sin \frac{2\pi}{25}(x - at)$$

for $x = x_{-2}$ and x_{-1}. We use this left boundary from the analytic solution for (3) in case both b and c zero, followed by initial condition $\eta(x, 0) = 0.1 \sin \frac{2\pi}{25} x$, see for example in [9]. The right boundary is absorbtion, i.e. we linearize two points η_{JJ}^{n+1} and η_{JJ-1}^{n+1} for η_{JJ+1}^{n+1}, also for η_{JJ+2}^{n+1}. Our numerical solution is given in Figure 2. We show the animation, the waves travel by decreasing the amplitude, as shown by plotting in 3-D. We calculate upto $t = 800$. This calculation can be continued for larger t. Plot of $\eta(x, 1200)$ is given in Figure 3 for curve with solid line. We can see the waves with smaller amplitude at the right side, after

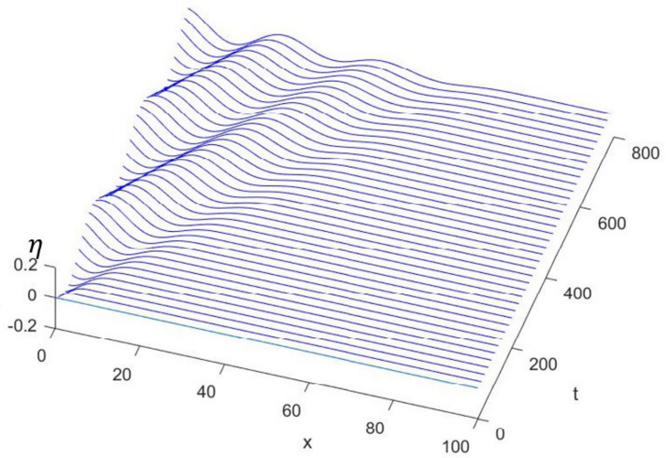

FIGURE 2. The numerical solution of (3), initial value $\eta(x,0)=0$ and left boundary $\eta(x,t)=0.1\sin\frac{2\pi}{25}(x-at)$

the incoming waves propagate to the right. The curve with dash-point (-.) is also given in Figure 3 as the plot of $\eta(x,1200)$ calculated using $\delta=0.7$. Here, we show the effect of the surface tension, larger value δ produces the incoming waves with reducing amplitude faster. Moreover, larger value δ also gives larger wave-number. This agrees with our analysis for monochromatic wave.

Wave deformation can also be observed from initial wave in form of solitary

$$\eta(x,0)=\sinh^2 0.5(x-25) \tag{5}$$

with zero left boundary condition. So, in it's propagating we can see the amplitude and also the form of the wave. We present the animation of that propagation in Figure 4. Here, we calculate (3) using $\theta=5^0$, $r=0.1$ and $\delta=0.1$. After running the numerical procedure upto $t=500$, we show the last profile $\eta(x,500)$ in Figure 5 (solid line) together with the plot using different $\delta=0.7$, dash-point curve (-.), and $\delta=0.9$, dash-dash curve (–). Smaller value δ produces slower declining the amplitude. This can be seen in Figure 5, with $\delta=0.1$ giving curve with slightly smallest amplitude after calculating upto the same time $t=500$.

The simulation so far uses various value of δ, without changing r, as δ involves only in the coefficient of fourth term in (3). It agrees to the analysis for monochromatic wave, δ contributes in decreasing the amplitude. Meanwhile, for various θ, it will effect to wave speed, as it is in the coefficient of the second term of (3). Increasing θ the wave travels faster, but reducing the coefficient of the third term in (3) resulting slower in decreasing the amplitude. This should be considered for δ so that the changing of the amplitude does not change. For monochromatic wave, it can be analyzed by the frequency *omega* and the wave number k. For

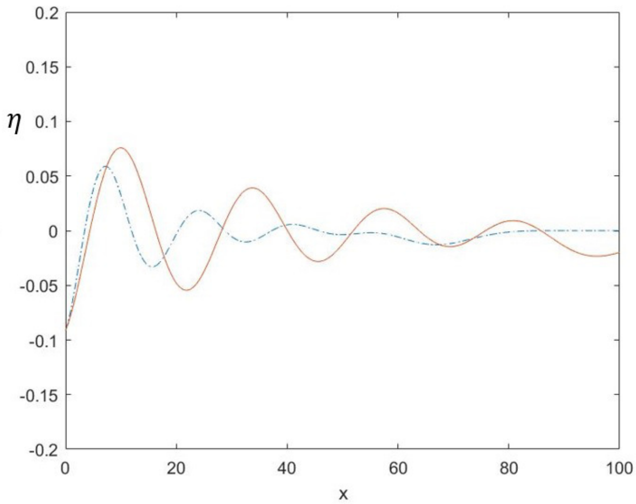

FIGURE 3. Plot of $\eta(x, 1200)$ after the incoming waves $\eta(x,t) = 0.1 \sin \frac{2\pi}{25}(x - at)$ propagating to the right following (3) for different δ, solid line corresponding to $\delta = 0.1$ and dash-point for $\delta = 0.7$

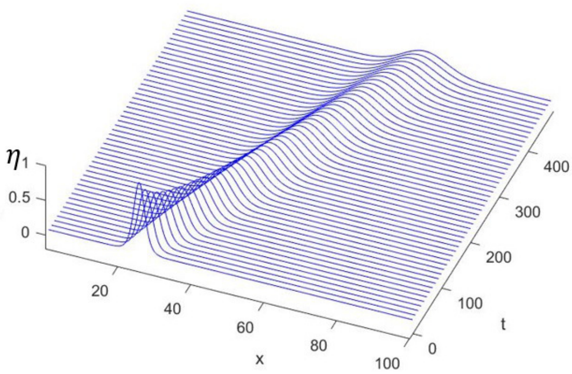

FIGURE 4. The numerical solution of (3), with initial value $\eta(x, 0) = \sinh^2 0.5(x - 25)$

other type of wave, it can be analyzed by numerical solution. To confirm those, we work for solitary wave. The initial wave (5) is used to determine the solution of (3), with $r = 0.1$, $\delta = 0.1$ and various θ. Plot of $\eta(x, 100)$ is shown in Figure 6 for

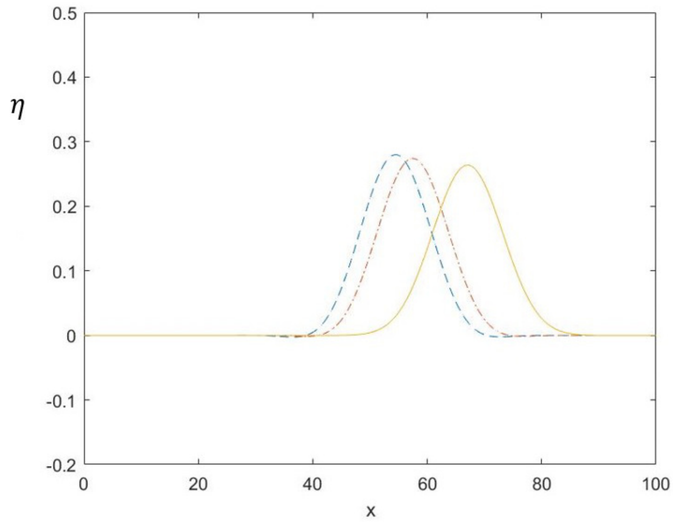

FIGURE 5. Plot of $\eta(x, 500)$ from initial value $\eta(x, 0) = \sinh^2 0.5(x - 25)$ with different $\delta = 0.1$ (solid curve) 0.7 (dash-point curve) and 0.9 (dash-dash curve)

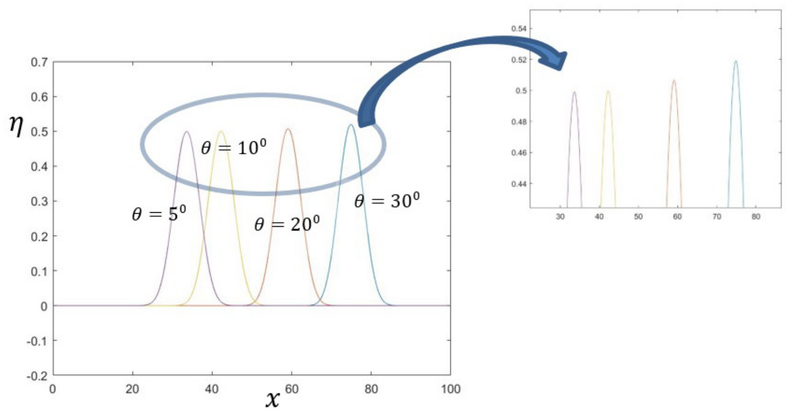

FIGURE 6. Plot of $\eta(x, 100)$ for different θ, that is $\theta = 5, 10, 20$ and 30 degree, from left to right. Enlargement is given at the top right side

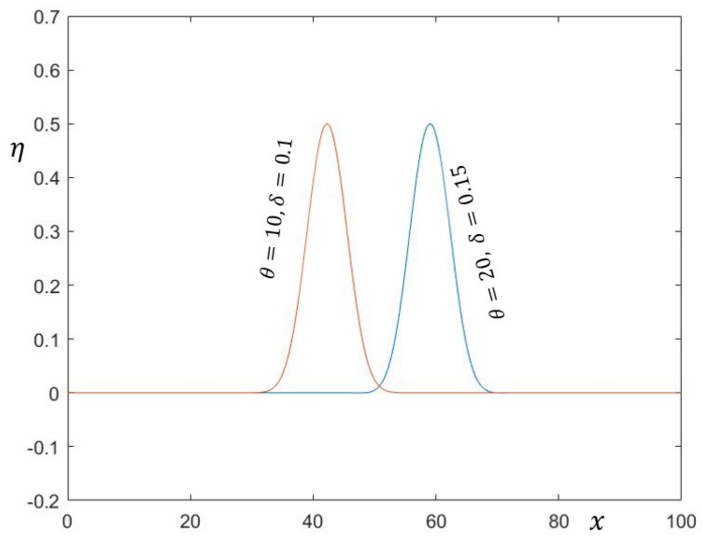

FIGURE 7. Plot of $\eta(x, 100)$ for $\theta = 10, \delta = 0.1$, and $\theta = 20, \delta = 0.15$ obtained from initial wave (5) and using $r = 0.1$

$\theta = 5, 10, 20$ and 30 degree as indicated, where the wave travels faster for larger θ. This can be seen by the position of the crest. It is followed by less reducing the amplitude. To see the difference of the amplitude for each θ is given the enlargement at the top right side of Figure 6. The maximum value of $\eta(x, 100)$ for $\theta = 30^0$ is largest between the other θ. This is proportional to the value of b in (3).

Now, we perform our calculation to get the same profile of the surface wave for different bottom inclination. We show in Figure 7, as the result of plot $\eta(x, 100)$ for $\theta = 10$ and $\theta = 20$. Both curves have the same profile with reducing the amplitude from initial wave (5), the maximum value of $\eta(x, 100)$ is 0.49977, but different position at $x = 42.2$ corresponding to $\theta = 10$ and at $x = 59.0$ for $\theta = 20$. To get those profiles, we need to adjust different value δ, that is 0.1 and 0.15 for the same value $r = 0.1$. From this performance, we can get the same wave profile from an initial wave by setting θ, r and δ, increase the inclination must be followed by increasing r.

5. CONCLUDING REMARKS

A linear model of thin film flow has been solved numerically. The model was developed from previous model by involving surface tension. Since the model was very thin and the evolution was very slow, scaling was needed. An implicit finite different method was chosen as it was unconditional stable, so that it could be used to observe the effect of the surface tension, that was fail using explicit method as it was conditional stable. Moreover, this numerical work was able to observe the model with general initial wave, not only monochromatic. We found that the surface tension contributes in reducing the amplitude during the wave propagates.

REFERENCES

[1] C. Pozrikidis, *Fluid dynamics: theory, computation, and numerical simulation.* Springer Science & Business Media, 2009.

[2] G. K. Batchelor, *An introduction to fluid dynamics.* Cambridge university press, 2000.

[3] L. H. Wiryanto and W. Febrianti, "Numerical solution of thin-film flowing down on an inclined channel," *Advances and Applications in Fluid Mechanics*, vol. 20, no. 4, pp. 595–604, 2017.

[4] A. King, E. Tuck, and J.-M. Vanden-Broeck, "Air-blown waves on thin viscous sheets," *Physics of Fluids A: Fluid Dynamics*, vol. 5, no. 4, pp. 973–978, 1993. https://doi.org/10.1063/1.858641.

[5] L. H. Wiryanto, R. Widyawati, R. Fauzi, G. Putra, and E. Noviani, "Simulation of wave propagation on thin film," *Advances and Applications in Fluid Mechanics*, vol. 29, p. 45–58, 2022. https://doi.org/10.17654/0973468622007.

[6] G. Putra, L. H. Wiryanto, and R. Widyawati, "An implicit finite difference method for thin film flow," *Journal of the Indonesian Mathematical Society*, vol. 29, no. 1, 2023. https://doi.org/10.22342/jims.29.1.1110.99-105.

[7] L. Wiryanto, "Stability analysis of thin film model," in *Journal of Physics: Conference Series*, vol. 983, p. 012072, IOP Publishing, 2018. https://doi.org/10.1088/1742-6596/983/1/012072.

[8] L. H. Wiryanto, "A finite difference method for a thin film model," 2017. http://www.e-jikei.org/Conf/ICMEMIS2017/proceedings/materials/proc_files/GS_papers/GS-02/Camera-readyICMEMIS_full_Rev.pdf.

[9] W. A. Strauss, *Partial differential equations: An introduction.* John Wiley & Sons, 2007.